PAWEŁ ŻAK, JANUSZ LELITO, JÓZEF S. SUCHY, WITOLD KRAJEWSKI, HALINA KRAWIEC, KATHARINA HABERL, PETER SHUMACHER, LINDSAY GREER, AMIR SHIRZADI, BEATA GRACZ

Modelling the effect of SiC particle size on crystallization of magnesium metal matrix composite; AZ91/SiC

INTRODUCTION

Grain size is one of the most important structural characteristic that determining mechanical properties. Knowing element properties, the proper application regions for it can be chosen to achieve best mechanical properties and performance. Nowadays simulation software can be use to predict the element microstructure. Those programs base on micro-macro model of crystallization. The model consists of partial differential equations (PDEs) that describe the nucleation rate, diffusion in the casting, casting cooling speed and every single grain growth rate. Often it is hard to find the theoretical value of the parameters that appear in those PDEs. It is possible to find them from experiment. The experimental data after applying statistical methods let us find approximated values of the so-called "fitting parameters" in the mentioned models [1÷4].

AZ91 alloy analyzed in this study is hypereutectic alloy. The magnesium primary α-Mg phase is dendritic. During crystallisation there appears eutectic reaction. In this study influence of eutectic is omitted because magnesium primary phase microstructure has most significant influence on mechanical properties of the casting.

MODEL DESCRIPTION

In the mathematical model it is assumed that heat transfer is governed by Fourier-Kirchhoff (FK) equation:

$$\frac{\partial T}{\partial \tau} = \frac{1}{c_p \rho} div(-\lambda grad T) + \frac{q}{c_p \rho}, \tag{1}$$

where: T, K – is temperature, τ, s – time; c_p, J·kg^{-1}·K^{-1} – specific heat, ρ, kg·m^{-3} – density, λ, W·m^{-1}·K^{-1} – thermal conductivity, $q = L(df_s/d\tau)$, W·kg^{-1} – heat of crystallization.

During simulation the temperature change speed is calculated. Its value consists of two parts: one, that depends on the temperature gradient and second that is phase change effect. In this article there is an assumption that simulation runs in one element of the melt. With this assumption the gradient depend part of FK can be expressed as a function of the actual temperature. The function was calculated from experimental data for the sand mold used in the experiment:

$$P(T) = \begin{cases} -40 & \text{for } T > 625^\circ C, \\ \frac{200}{T-630} & \text{for } 625^\circ C \geq T > 620^\circ C, \\ \frac{5T-2900}{T-630} & \text{for } 620^\circ C \geq T > 600^\circ C, \\ \frac{100}{T-630} & \text{for } T \leq 600^\circ C. \end{cases} \tag{2}$$

The heat of crystallization is calculated using micro-macro model of crystallization. The proposed model taking into account the influence of new grains forming in the liquid and their effect on the chemical constituents field. It is assumed that the α-Mg phase grain growth is controlled by aluminium diffusion coupled with temperature distribution. The grains are assumed to be spherical. Second Fick's law, mass balance and interface moving speed describe Al concentration change rate along the grain radius and in the surrounding liquid. The difficulty implied by moving interface was overcome by employing the Murray-Landis correction to Fick's law [5]. For the liquid and already solidified α-Mg phase grain the governing PDEs:

– α-Mg phase:

$$\frac{dC}{d\tau} = D_{Al}^{\alpha}\left(\frac{\partial^2 C}{\partial r^2} + \frac{2}{r}\frac{\partial C}{\partial r}\right) + \frac{r}{R}\frac{\partial C}{\partial r}\frac{dR}{d\tau} \tag{3}$$

liquid:

$$\frac{dC}{d\tau} = D_{Al}^{L}\left(\frac{\partial^2 C}{\partial r^2} + \frac{2}{r}\frac{\partial C}{\partial r}\right) + \frac{R_{inf}-r}{R_{inf}-R}\frac{\partial C}{\partial r}\frac{dR}{d\tau} \tag{4}$$

where: C denotes dimensionless Al concentration; D, m^2·s^{-1} with adequate superscript denotes diffusion in the grain radius (α) and in the liquid (L), r, m – distance from the grain center; R, m – interface distance from the grain center, R_{inf}, m, is maximal possible radius.

The equations presented above (3, 4) consist of two components: one is second Fick's law, second describes influence of interface moving speed on the chemical composition. The Al concentration in the grain and in the surrounding liquid determine grain growth speed:

$$(C_L - C_S)\frac{dR}{d\tau} = D_{Al}^{\alpha}\left.\frac{dC}{dr}\right|_{R^-} - D_{Al}^{L}\left.\frac{dC}{dr}\right|_{R^+} \tag{5}$$

where: C_L – Al liquidus concentration for actual temperature, C_S – Al solidus concentration for actual temperature.

Above equations (3÷5) are analogous to those presented in [6, 7]. In this article the continuous nucleation is taking into account. The grains start appear at the liquidus temperature and continue until the end of the nucleation temperature is reached. This temperature is calculated as a temperature at which the temperature starts to grow (recalescence) or is constant. The already appeared grains grow in accordance with formulas (5, 3, 4), after the nucleation stops, the grains still grow in the same way.

Grain nucleation rate was calculated with Fras [4] model. This is immediately nucleation model – grain number depends on the maximal undercooling – but in this article it was transformed into the form that depends on the temperature. Another modification was made by taking into account its dependence on the SiC particles size. The modified Fras nucleation model has a form:

$$N_V(T, d_{SiC}) = \lambda(d_{SiC})\exp\left(-\frac{b(d_{SiC})}{(T_N - T)}\right) \tag{6}$$

where: T, K, is actual temperature, d_{SiC}, m, is the particles mean diameter, λ, m^{-3}, b, K, denotes model adjustment parameters, T_N – is nucleation temperature. Nucleation temperature can be described with the function that depends on mass fraction of the ceramic particles in the composite.

M.Sc. **Paweł Żak** (pawelzak@agh.edu.pl), Ph.D. **Janusz Lelito**, Prof. **Józef S. Suchy**, Prof. inż. Witold Krajewski, Ph.D. **Halina Krawiec**, M.Sc. **Beata Gracz** – Faculty of Fundry Engineering, AGH University of Science and Technology, Krakow, M.Sc. **Katharina Haberl**, Prof. **Peter Shumacher** – Chair of Casting Research, University of Leoben, Austria, Prof. **Lindsay Greer** – Department of Materials Science and Metallurgy, University of Cambridge, UK, Ph.D. **Amir Shirzadi** – Materials Engineering, The Open University, UK and Department of Materials Science and Metallurgy, University of Cambridge, UK

During each time step of the simulation there appear specific number of nuclei. In this model there are gather in the structure named class of grains. Each grain in the class have the same radius, and Al concentration at the radius for them is the same. For each time step the volume of representative grain of each class is calculated, than the volume is multiplied by the number of the grains gathered in the class, partial volume values for the grain classes are summarized to obtain total solid volume. The value by which the total volume increasing gives the latent heat release value.

To find the adjustment parameters in model presented above experimental castings of AZ91/SiC was performed.

EXPERIMENTAL PROCEDURE

Composite casting

The composite with AZ91 (Tab. 1) metal matrix and SiC reinforcement particles was prepared. Three castings were prepared for different SiC particles size, the sizes were: A – 10 μm, B – 40 μm, C – 76 μm. During each casting 6000 g of the AZ91 alloy was used. Different weight percentage of SiC particles: 0, 0.1, 0.5, 1, 2, 3.5 wt. % were used to prepare different composites. The samples were casted into standard thermoanalysis croning sand cup with thermocouple K-type. The specimens were taken from the region near to the thermocouple. Thermoanalysis data was used for cooling speed and under-cooling determination for each sample.

Etching

The specimens were then cut, ground and polished with the grinding machine. Etching of the specimens was performed according to the procedure described by the Maltais [8, 9] and improved by authors [10]. The chemical composition of etchant was: 50 ml Distilled Water, 150 ml Ethanol, 1 ml Acetic Acid.

The specimens were immersed in etching solution for 80÷95 s. They were then rinsed in ethyl alcohol and put dried from 50 cm with a blast of room-temperature air. During this stage specimens were gently moved so the remaining liquid still wet their surface.

The etched specimens were examined using a light microscope Carl Zeiss AXIO Imager A1 with cross polarized light and λ filter. The images on computer display reveals arms of different dendritic grains as areas with different colours.

Grain density measurement

Data gathered from light micrographic analyse was then used to calculate the grain density N_V. To find this value from analysis data, the Saltykov [11] equation can be used:

$$N_V = \frac{2}{\pi} N_a \left(\frac{1}{d}\right)_{mean} \tag{7}$$

where: N_V, m^{-3}, is mean volumetric grain density, N_a, m^{-2}, is mean grain density on the surface, and $(1/d)_{mean}$, m^{-1}, denotes average value of $(1/d)$, m^{-1}, for all grains found on the polished section.

RESULTS

Mean grain volumetric density

Mean grain density measurement results are gathered in Figure 1. The calculations were made after Saltykov formula (7). It can be seen from this picture that mean grain density increasing while more particles were put into the alloy. The grains in the composites reinforcement with smaller particles (10 μm) are smaller than for composites with bigger particles. Also in the case of 10 μm particles even for not so big amount of SiC particles large refinement effect can be observed (Fig. 1). The mean grain density in the 10 μm particles case of 0.1÷2 wt. % content is approximately one rank of magnitude greater than in the case of SiC particles 40 and 76 μm large.

Table 1. Chemical composition of AZ91 alloy, wt. % determined using ICP-OES VARIAN Vista MPX

Tabela 1. Skład chemiczny stopu AZ91, w procentach masowych, wyznaczony za pomocą ICP-OES VARIAN Vista MPX

Al	Zn	Mn	Fe	Be	Si	Cu	Ni
8.5	0.64	0.23	<0.002	10 ppm	0.03	0.003	0.001

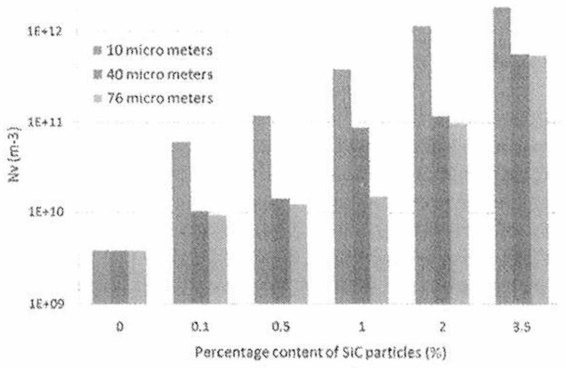

Fig 1. Mean grain density dependence on size and content of reinforcement SiC particles, logarithmic scale

Rys. 1. Zależność średniej gęstości ziaren od udziału oraz rozmiaru cząstki zbrojącej SiC, skala logarytmiczna

Adjustment parameters

Thermoanalysis data and micrographics results were used to find nucleation temperature for composites with different amount of SiC particles and fitting parameters in nucleation model (6). To fit the theoretical curve with experimental data the Statistica 8.0 and Origin 8.0 Pro were used.

It was not noticed during thermoanalysis that the size of particles have any influence on nucleation temperature. However the nucleation temperature changes as the content of SiC particles growing. It was observed that this growth can be described with the functional dependence:

$$N_V\left(mf_{SiC}\right) = 881 - 5.9\exp\left(-91.9mf_{SiC}\right), \quad [K]. \tag{8}$$

The curve described by equation (8) and experimental data are shown in the Figure 2.

The Figure 2 shows very good correlation between experimental and model data. The calculated with equation (8) value of nucleation temperature was then used during nucleation and crystallization phenomena simulation.

The experimental data of grain density and undercooling measurement was used to find adjustment parameters in nucleation model (6). At the beginning the grain density dependence on the undercooling for each particles size was taken into account. As a result of this analysis three formulas were determined:

– N_V on undercooling dependence for 10 μm particles:

$$N_V(T) = 1.7 \cdot 10^{14} \exp\left(-\frac{43.21}{T_N - T}\right), \tag{9}$$

$$R^2 = 0.993,$$

– N_V on undercooling dependence for 40 μm particles:

$$N_V(T) = 3.9 \cdot 10^{15} \exp\left(-\frac{93.83}{T_N - T}\right), \tag{10}$$

$$R^2 = 0.984,$$

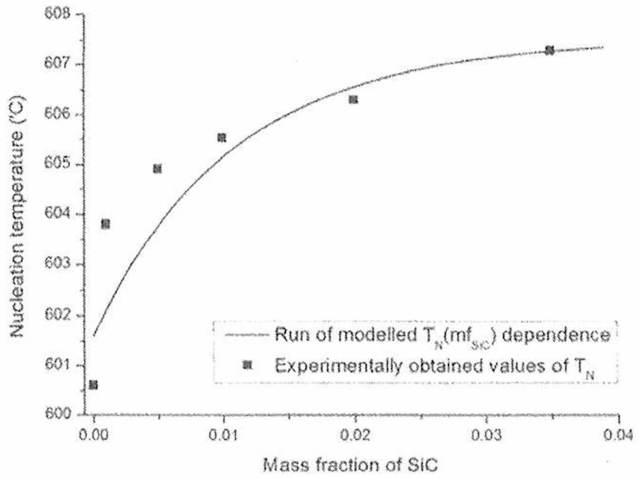

Fig. 2. Statistically fitted nucleation temperature dependence on SiC mass fraction and experimental analysis results
Rys. 2. Statystycznie dopasowana krzywa opisująca zależność temperatury zarodkowania od udziału masowego cząstek SiC oraz wyniki pomiarów eksperymentalnych

– N_V on undercooling dependence for 76 μm particles:

$$N_V(T) = 9.4 \cdot 10^{16} \exp\left(-\frac{135.09}{T_N - T}\right), \quad (11)$$

$$R^2 = 0.999.$$

It is obvious that because of the simulation conditions, value of T in above equations (9÷11) is lower than T_N.

The value of λ, b parameters in nucleation model depends also on the SiC particles size d_{SiC}. As an effect of statistical analysis the formula that connects undercooling and reinforcement particles size influence on the volumetric grain density was obtained:

$$N_V(T, d_{SiC}) = 9.1 \cdot 10^{14} \exp\left(3.1 \cdot 10^4 - \frac{32.6 + 1.4 \cdot 10^6 d_{SiC}}{T_N - T}\right), \quad (12)$$

$$R^2 = 0.932.$$

This equation makes performing the nucleation and solidification simulation for AZ91/SiC composites of different size of SiC particles possible.

Simulation

The model described above eq. (1÷6, 8, 12) was used to prepare computer simulation software. It was written in *C++* language in Microsoft Visual Studio Environment. During the simulation temperature of the single element of the liquid was calculated. The cooling speed in F-K equation, resulting from temperature gradient in domain, was calculated with function (2). The initial temperature for the process was 700°C. T_N was calculated with equation (8). The diffusion coefficient for the α-Mg: $D_{Al}^{\alpha} = 2.7 \cdot 10^{-10}$, m/s², for the AZ91 melt: $D_{Al}^{L} = 2.7 \cdot 10^{-8}$, m/s². Thermophysical parameters of AZ91 were assumed to be constant with the temperature. Maximal possible radius for the grain in the class was calculated with following formula:

$$R_{int} = \sqrt[3]{\frac{3(1-V)}{N}}, \text{ m} \quad (13)$$

where: V, m³, denotes already solidified volume and N is number of grains in the class.

Results of the simulation were later validated with experimental casting. The simulation run for AZ91/SiC composite of 2% content of SiC, $d_{SiC} = 45$ μm, showed very good correlation with experimental data (Fig. 3).

The results of the simulation are quite similar to the experimental data. Especially at the beginning, for about first 125 s of the process the curves are almost identical.

During computations the end of nucleation is calculated. After this temperature no more grains appears in the melt. This feature of analysed model makes it possible to predict the grain density after solidification. In the presented case measured grain density $N_V = 1.2 \cdot 10^{11}$, and simulated grain density was $2 \cdot 10^{11}$. Both values are at the same order of magnitude. It is possible that the simulated value can be closer to real values if the neighbour elements could change the cooling speed. As the cooling rate was given explicite there is no such influence.

In the Figure 4 the grain density growth in time can be observed. It can be seen that the nucleation phenomenon least quite short: about 10 s. Another interesting thing is that at the end of the nucleation its rate getting smaller, the curve smoothly changes in horizontal line that represent the maximal grain density. In the Figure 5 the grain density growth with temperature decreasing can be observed. In this picture it can be seen that the grain density grows linearly if $T \in (596°C; 604°C)$. At the ends this line changes smoothly into horizontal lines that represent 0 and maximal calculated grain density.

At the time of simulation the volume increments are calculated. Summation of those increments give the actual solidified volume. Actual solidified volume divided by total element volume gives the solid fraction value. The diagram of solid fraction growth is presented in Figure 6.

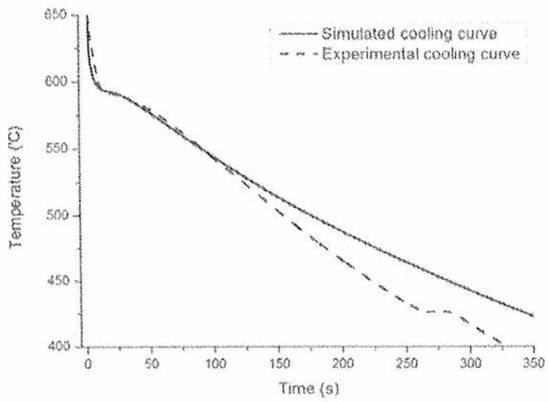

Fig. 3. Simulated and experimental cooling curve comparison
Rys. 3. Porównanie krzywej stygnięcia eksperymentalnej oraz uzyskanej dzięki symulacji

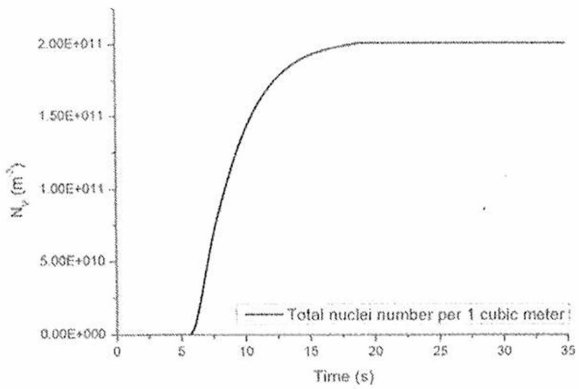

Fig. 4. Grain density growth versus time
Rys. 4. Zmiana gęstości ziaren w czasie

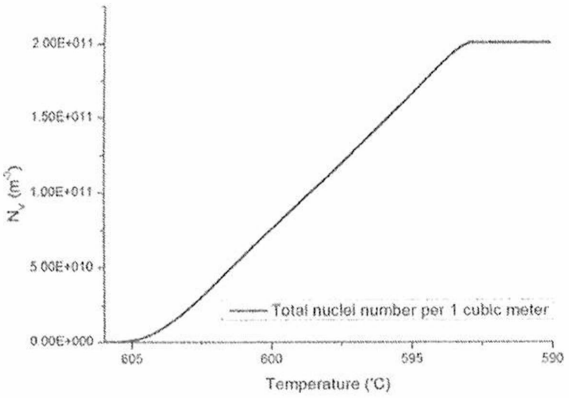

Fig. 5. Grain density versus actual alloy temperature
Rys. 5. Zmiana gęstości ziaren w funkcji temperatury stopu

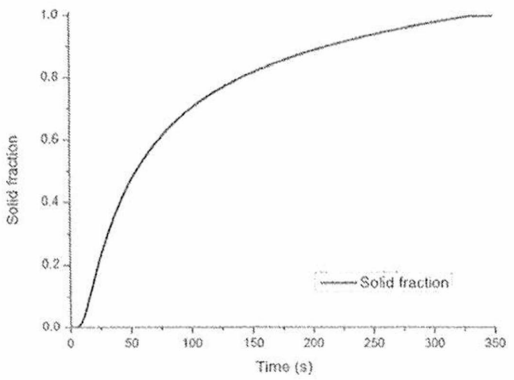

Fig. 6. Solid fraction change versus time
Rys. 6. Zmiana udziału objętości zakrzepłej w czasie

This diagram shows that the solid fraction grows very fast at the beginning of the crystallization phenomenon and than its speed slows. The line smoothly goes to the horizontal line that represent the situation when total amount of the liquid is already solidified.

CONCLUSIONS

The experimental data can be used to prepare micro-macro composite crystallization model. The model fits good with an experiment results. The differences are probably connected with the assumptions that were made during model preparation and with the fact, that simulation was performed just for one element of the composite.

Numerical simulation gives a lot of useful data that can give new view on the nucleation and solid fraction growth phenomenon. This knowledge can be later used to influence those processes.

SiC particles have refinement effect on the composite microstructure. The smaller particles give finer microstructure. The biggest change of the grain density can be observed in composite versus pure AZ91 alloy, even if the amount of the particles is not so large.

ACKNOWLEDGEMENTS

The authors acknowledge The European Community for financial support under Marie Curie Transfer of Knowledge grant No. MTKD-CT-2006-042468 (AGH No. 27.27.170.304) and Polish Ministry of Science and Higher Education for financial support under grant No. N507-44-66-34 (AGH No. 18.18.170.325).

REFERENCES

[1] Asthana R.: Solidification processing of reinforced metals. Key Engineering materials 151-152 (1998).
[2] Luo A.: Heterogeneous nucleation and grain refinenent in cast Mg(AZ91)/SiC metal matrix composites. Canadian Metallurgical Quaretly 35 (1996), 375-383
[3] Lelito J., Zak P., Suchy J. S.: The grain nucleation rate of AZ91/SiC composite based on Maxwell-Hellawell model. Archives of Metallurgy and Materials 54 (2009) 347-350.
[4] Fras E., Wiencek K., Gorny M., Lopez H.: Theoretical model for heterogeneous nucleation of grains during nucleation. Material Science and Technology 19 (2003) 1653-1659.
[5] Fromm J. E.: An introduction to computer simulation in applied science. Abraham F. A. and Tiller W. A., eds. Palo Alto Scientific Center Raport No. 320-3269 (1970).
[6] Kapturkiewicz W., Fras E., Burbelko A.: Computer simulation of the austenitizing process in cast iron with pearlitic matrix. Materials Science and Engineering A 413-414 (2005) 352-357.
[7] Johnson W. C., Heckel R. W.: Mathematical modeling of diffusion during multiphase layer growth. Metallurgical transactions 12 (1981) 1693-1697.
[8] Maltais A., Dube D., Fiset M., Laroche G., Tugeon S.: Improvements in the metallography of as-cast AZ91 alloy. Materials Characterization 52 (2004) 103-119.
[9] Maltais A., Dube D., Roy F., Fiset M.: Optical anisotropy of a color-etched AZ91 magnesium alloy. Materials Characterisation 54 (2005) 315-326.
[10] Zak P., Lelito J., Shumcher P., Haberl K., Krajewski W., Suchy J. S.: Color etching of AZ91/SiC composite. XXXIII Konferencja naukowa z okazji Święta Odlewnika, Kraków, Poland 11 grudnia 2009. http://www.odlew.agh.edu.pl/inne/konferencje/dzien_odlewnika_2009.html.
[11] Cybo J., Jura S.: Funkcyjny opis struktur izometrycznych w metalografii ilościowej (in Polish). Wydawnictwo Politechniki Śląskiej, Gliwice (1995).